Konrad-Zuse-Zentrum
für Informationstechnik Berlin

Takustraße 7
D-14195 Berlin-Dahlem
Germany

MANON BONDOUY AND SUSANNA RÖBLITZ

Mathematical modeling of follicular development in bovine estrous cycles

ZIB-Report 12-26 (August 2012)

Herausgegeben vom
Konrad-Zuse-Zentrum für Informationstechnik Berlin
Takustraße 7
D-14195 Berlin-Dahlem

Telefon: 030-84185-0
Telefax: 030-84185-125

e-mail: bibliothek@zib.de
URL: http://www.zib.de

ZIB-Report (Print) ISSN 1438-0064
ZIB-Report (Internet) ISSN 2192-7782

Mathematical modeling of follicular development in bovine estrous cycles

Manon Bondouy [*] Susanna Röblitz [*†]

August 6, 2012

Abstract

Normal follicular development is a prerequisite for successful fertilization in dairy cows. During the last decades, however, prevalence of anestrus has been increasing for different reasons. In this study we use a mathematical model to investigate mechanisms that lead to anestrus. This model is derived by coupling two previously published models: a small model for the development of multiple follicles (Smith et al., 2004), and a large estrous cycle model (Stötzel et al., 2012). We first investigate the influence of synchronization protocols on the time-shift of ovulation. In a second scenario we simulate an extended period of anestrus as it typically occurs after calving.

AMS MSC 2000: 90C31, 92C30, 92C42, 93A30

Keywords: ordinary differential equations, systems biology, reproduction, dairy cows

[*]Zuse Institute Berlin, Takustraße 7, 14195 Berlin, Germany
[†]Corresponding author. E-mail: susanna.roeblitz@zib.de

Contents

Introduction

Concurrent with selection for increased milk yield, a decrease in dairy cow fertility has been observed during the last decades [14]. This decline in fertility is shown by, e.g., alterations in hormone patterns during the estrous cycle, reduced expression of estrus behavior and lower conception rates [19]. However, the antagonistic relationship between milk yield and reproductive performance is a multifactorial issue [5]. New strategic directions for genetic selection including fertility-related traits will take time to be effective. In the mid-term, mathematical modeling of the involved mechanisms is expected to improve insight into the biological processes underlying the bovine estrous cycle, and could thereby help to develop strategies against declined fertility in dairy cows.

Although the endocrine and physiologic regulation of the bovine estrous cycle is studied extensively, mathematical models of cycle regulation are scarce and of limited scope [11, 16]. A number of models have been developed for other ruminant species, especially ewes [6, 9], but these models do not contain all the key components that are required to simulate follicle development and the accompanying hormone levels throughout consecutive cycles. In a cooperation between scientists from ZIB and animal scientists from Wageningen, a new model was developed that integrates the major tissues and hormones involved in the dynamics of follicular development [4]. This model served as a basis for the examination of follicular wave patterns [3], as well as for the study of synchronization protocols [18]. It includes the processes of follicle and corpus luteum (CL) development and the key hormones that interact to control these processes: gonadotropin-releasing hormone (GnRH), luteinizing hormone (LH), follicle stimulating hormone (FSH), estradiol (E2), progesterone (P4), oxytocin (OT), and prostaglandin F2α (PGF2α). This model generates successive estrous cycles with a varying number of follicular waves per cycle. Follicular development is modeled with a single equation that represents the state of follicular maturation and the ability of follicles to produce steroid hormones.

Two other models have been published by Soboleva et al. [16] and Smith et al. [15]. These two models are very similar in that they both describe the growth of many follicles by using one equation for each follicle. Large follicles suppress the growth of small ones, thus giving rise to usually one dominant follicles. The model in [16] describes ovarian follicular development following commitment throughout one follicular wave. The model in [15] additionally describes the interaction among follicles, LH, FSH, and E2. This model has especially been constructed to simulate postpartum anestrus. Hence, simulations stop with ovulation and do not depict sequences of ovulatory cycles.

The aim of this study is to couple these models in order to simulate the development of multiple follicles throughout consecutive cycles. The paper is organized as follows. We start with an explanation of the biological background in Section 1. Thereafter, Section 2 briefly describes the models in [18, 15, 16], before we derive a new submodel in Section 3. In Section 4, we present the coupling between this new sub-model and the large estrous cycle model from [18]. Simulation results for synchronization protocols and postpartum anestrus are discussed in Section 5.

1 Biological background

The usual length of an estrous cycle is about 21 days. The cycle can be divided into four periods, which are separated according to hormone levels in the blood: estrus, met-estrus, di-estrus, and pro-estrus. Ovulation is regulated by the interplay of various reproductive hormones.

1.1 The phases of an estrous cycle

Estrus refers to the phase when the female is sexually receptive. Since the corpus luteum underwent lysis earlier in time, the progesterone level in the blood is very low. E2 levels are decreasing from the high levels that were reached just prior to estrus. Finally, LH spikes to a high level during estrus, which initiates ovulation. During *met-estrus*, the corpus luteum starts to form. It is still small and does not yet have the capacity to produce large amounts of progesterone at this stage of development. Therefore, progesterone levels are still low, but increase slightly during met-estrus. *Di-estrus* is characterized by the activity of the corpus luteum and the production of large amounts of progesterone. Small follicles emerge from a cohort of antral follicles, but do not proceed further. *Pro-estrus* is characterized by regression of the CL and deviation of an ovulatory follicle. The follicle matures under the influence of FSH and pulsatile LH, secreted from the pituitary. FSH plays an important role in the beginning of follicular growth, whereas LH is important for maturation up to ovulation. Pro-estrus and estrus form the *follicular phase*, whereas met-estrus and di-estrus make up the *luteal phase*.

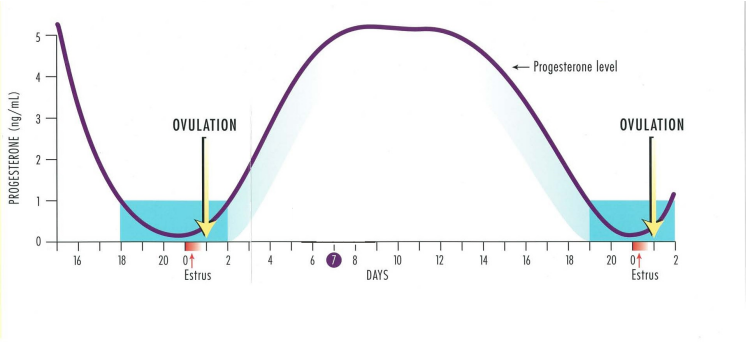

Figure 1: Progesterone level and ovulation [10]

1.2 Reproductive hormones

The hypothalamus controls the release of pituitary hormones by releasing small peptide hormones that travel down along short blood vessels from the hypothalamus to the pituitary. In particular, the hypothalamic hormone GnRH causes

the pituitary to release LH and FSH. Other hypothalamic hormones either inhibit or induce the release of additional pituitary hormones (growth hormone, ACTH, TSH, MSH and prolactin). These hormones have some affect on reproduction, but we will focus on FSH and LH because they more directly regulate the estrous cycle. Estradiol and progesterone have a negative feedback on the hypothalamus.

Corpus Luteum and progesterone The LH surge induces ovulation and differentiation of cells of the follicular wall into luteal cells [12]. The primary purpose of the CL is to produce P4. In general, as the CL increases in size at the beginning of the luteal phase, progesterone production also increases. As long as P4 levels are high, the ovaries continuously show follicular growth and decay in a dynamic wave pattern up to the deviation phase, but ovulation is inhibited. When the progesterone level is low, ovulation can occur (Figure 1).

Follicular waves and follicle stimulating hormone The follicular growth is not linear, but occurs in waves (about 3 waves per cycle). Under the influence of FSH, a cohort of 8-41 growing follicles emerge [1]. From this group of follicles, one follicle is allowed to grow to a much larger size than the others. This large follicle is called the dominant follicle, because it has the ability to regulate and restrict the growth of the smaller follicles. A few days after reaching maximum size, the dominant follicle begins to degenerate and dies. As the dominant follicle degenerates, its ability to restrict the other follicles is reduced. Therefore, if FSH levels are high enough, a new follicular wave is initiated. As a consequence of this dynamic process, follicles of all sizes exist on each day of the estrous cycle. The large follicle that eventually ovulates is identifiable on the ovary only 48 hours before estrus.

Estradiol As follicles grow they produce increasing amounts of estradiol. Circulating concentrations of estradiol increase and decrease as follicular waves grow and regress.

Luteinizing hormone The main function of LH is to trigger ovulation, thereby releasing an egg from the dominant follicle, and to initiate the conversion of the residual follicle into a corpus luteum.

2 Description of previous models

In the following we briefly describe the large estrous cycle model with a single follicle equation [18] and the two smaller models for multiple follicles [15, 16], which form the basis for the coupled model later on.

2.1 A large model: The model by Stötzel et al.

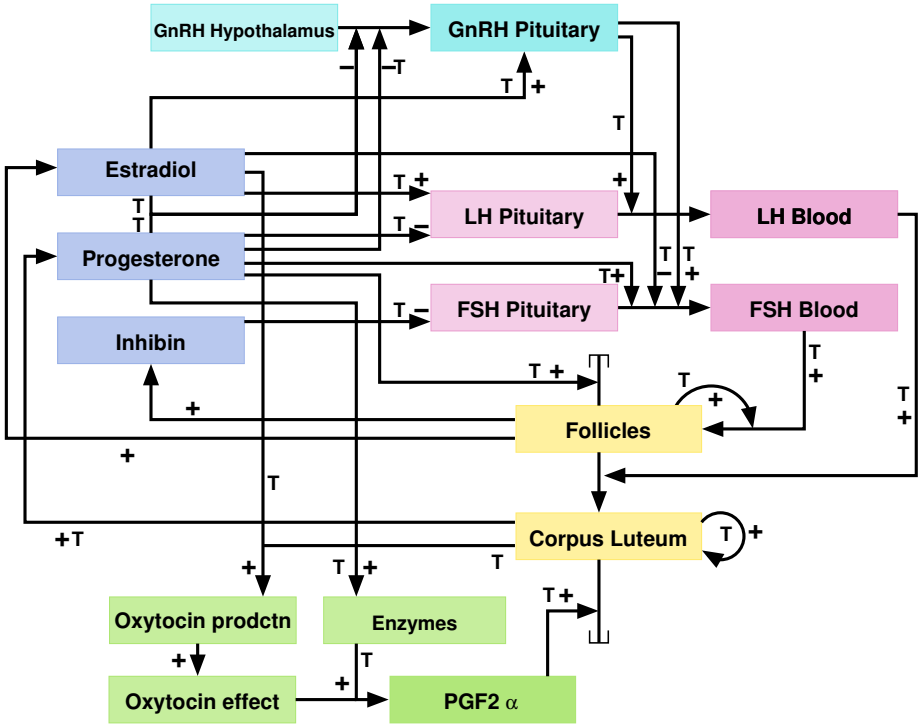

Figure 2: Mechanisms of the large bovine estrous cycle model published in [18]. Boxes represent the 15 key components of the system. Differential equations are derived for these 15 components. Arrows denote functional dependencies. Stimulating and inhibiting effects are indicated by $+$ and $-$, respectively. T represents a threshold.

A large model for the bovine estrous cycle has been published in [18]. Its mechanisms are illustrated in Figure 2. The model comprises 15 ordinary differential equations and generates hormone profiles of successive estrous cycles with several follicular waves per cycle. It describes the growth and decay of follicles and corpus luteum, as well as the change of the key reproductive hormones and enzymes over time. The model has been validated with data from synchronization studies.

Although this model takes into account several interactions between hormones, it has the disadvantage of only simulating the accumulative behavior of the follicles. Therefore we considered more detailed but smaller models that describe the dynamics of many follicles at the same time [16, 15].

2.2 A small model: The model by Smith et al.

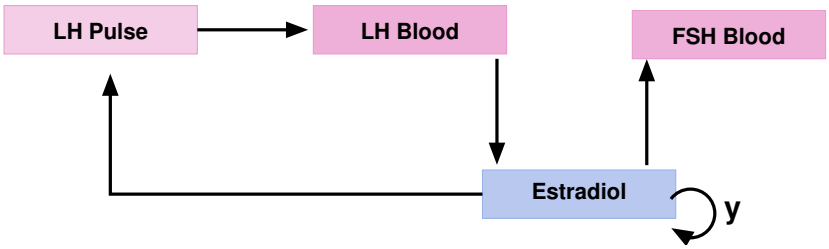

Figure 3: Schematic outline of the hormonal interactions in the model by Smith et al.

The model in [15] describes the dynamics of many follicles at the same time and their interactions with LH and FSH. Follicular size is modeled indirectly via E2 production per follicle. The model does not account for the time after ovulation and the influence of progesterone. Figure 3 depicts the interactions in this model, which are described by the following equations:

- FSH

$$\frac{d}{dt}FSH(t) \quad = \quad \beta \cdot FSH \cdot \left(\beta_1 - \frac{d}{dt}\max(x_i)\right) \tag{1}$$

- E2 production (x_i is the estradiol produced by follicle i, $i = 1, 2, \ldots, N$)

$$\frac{d}{dt}x_i(t) \quad = \quad k \cdot x_i \cdot (1 - x_i) \cdot [y + \kappa \cdot LH - (\mu - x_i) \cdot \sum_{j=1}^{N} x_j] \tag{2}$$

- Sensitivity of the hypothalamus to E_2

$$\frac{d}{dt}y(t) \quad = \quad -\frac{a \cdot (\max(x_i) - \text{mean}(x_i))}{1 + b \cdot t} \tag{3}$$

- LH

$$\frac{d}{dt}LH(t) \quad = \quad l \cdot \nu_p^+ - c \cdot LH \quad , \nu_p^+ = \begin{cases} \nu_p, & \nu_p \geq 0 \\ 0, & \nu_p < 0 \end{cases} \tag{4}$$

- Pulse generator

$$\frac{d}{dt}\nu_p(t) \quad = \quad A\left(1 - \frac{\alpha}{1 + b \cdot t}\right)\left(\frac{1}{1.01 - \max(x_i)}\right) \cdot \sin(p) \tag{5}$$

$$\frac{d}{dt}p(t) \quad = \quad \nu_p \tag{6}$$

Parameters Parameters β and β_1 characterize the rate of FSH increase and decrease. The function $y + \kappa \cdot LH$ supports follicular development. A follicle ovulates if this function approaches μ^2, whereby μ describes the rate of E2 production by each follicle. κ characterizes the sensitivities of the ovaries to LH. The parameter b determines the decrease in y, until y becomes low enough for ovulation. Parameters l, A and α describe the amplitude of LH pulses, and c is the degradation rate of LH.

Functionality FSH does not have a direct influence on the other equations, but it triggers an event: Whenever the level of FSH reaches some threshold, a new commitment begins. y and FSH are re-set to their initial values. Moreover, the number of follicles and the initial values of x_i are selected randomly and independently for each new wave. The corresponding distributions are not given in [15]. A follicle is considered to reach ovulation after many waves when $x_i = 1$.

Results Unfortunately, the publication [15] does not contain information on the initial values of the species. The value of the FSH-threshold is missing as well. When we tried to re-implement the model and to identify initial values from published simulation results, we figured out that the simulation results are very sensitive with respect to the initial values. Hence our results were not conclusive. In particular, a high LH frequency challenges any adaptive stepsize control, and we obtained different results with different numerical integrators (MATLAB's `ode45` and `ode23s`). Therefore we decided to go one step back and to implement a simpler model that was published five years earlier [16].

2.3 A tiny model: The model by Soboleva et al.

A dynamic model to describe ovarian follicular development following commitment has been developed in [16]. Follicular development is described by a series of i equations ($i = 1, 2, \ldots, N$),

$$\frac{d}{dt}x_i(t) \quad = \quad \frac{k \cdot \lambda^2}{E} \cdot x_i \cdot (E - x_i) \cdot [\lambda^2 - (\lambda - x_i) \cdot \sum_{j=1}^{N} x_j] \tag{7}$$

where x_i is the amount of E2 produced by the ith follicle.

Parameters The rate of estradiol production by each follicle is described by λ. The term $\lambda^2 - (\lambda - x_i) \cdot \sum_{j=1}^{N} x_j$ describes the interaction among the follicles. The parameter k is a measure of time. The factor $k \cdot x_i \cdot (E - x_i)$ describes the logistic law of growth, with E as maximum level of estradiol.

Functionality As in the model by Smith et al., follicular growth is identified with estradiol production, and in a group of follicles the dominant follicle suppresses the growth of the smaller ones. Note that with this model only one wave can be simulated, which usually ends with ovulation. Different initial conditions can lead to single ovulation, multiple ovulations, or even an anovulatory wave. In addition, the model in [16] was modified slightly to describe the effect of exogenous FSH on the development of follicles.

Results We were able to reproduce the results published in [16]. Since we are still interested in simulating multiple follicular waves, we will in the next step combine the two models [15] and [16] and extend them towards the interaction with endogenous FSH and P4.

3 A submodel with multiple follicles

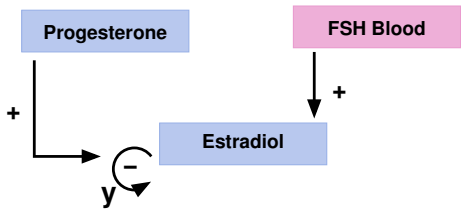

Figure 4: Schematic outline of the hormonal interactions in our model. Stimulating and inhibiting effects are indicated by + and −, respectively.

Figure 4 depicts the interactions that we want to include in our model. FSH and P4 are modeled as input curves (Figure 5), which represent the typical change of these hormones in the blood over time.

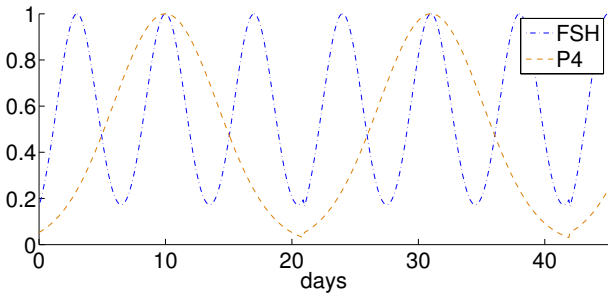

Figure 5: FSH and P4 input curves.

3.1 Model equations

FSH and P4 are added into the equations for follicular growth via hill functions as in [4]. A new follicular wave is initialized if one of the two following events occurs: either all follicles undergo atresia or at least one follicle becomes large enough. In this case the integration is re-started with new initial values of every follicle, and y is re-set to its initial value.

- FSH and P4 input functions

$$\begin{aligned} FSH(t) &= \exp(-(\mathrm{mod}(t,21)-3)^2/5) + \exp(-(\mathrm{mod}(t,21)-10)^2/5) \\ &\quad + \exp(-(\mathrm{mod}(t,21)-17)^2/5) + \exp(-(\mathrm{mod}(t,21)-24)^2/5) \quad (8) \\ P4(t) &= \exp(-(\mathrm{mod}(t,21)-10)^2/34) \quad (9) \end{aligned}$$

- Follicular maturation

$$\frac{d}{dt}x_i(t) = \frac{k\cdot\lambda^2}{E}\cdot\frac{FSH(t)^5}{T^5+FSH(t)^5}\cdot x_i\cdot(E-x_i)\cdot[y-(\lambda-x_i)\cdot\sum_{j=1}^{N}x_j] \quad (10)$$

- Sensitivity of the hypothalamus to E_2

$$\frac{d}{dt}y(t) = -\frac{a \cdot [\max(x_i) - \text{mean}(x_i)]}{1 + \frac{b}{P4(t)^2}} \tag{11}$$

Parameters and initial values Table 1 contains parameters and initial values used for the simulations.

Parameter	Value
k	$4.0725 \cdot 10^{1}$
μ	$5.47611 \cdot 10^{-1}$
a	$7.12 \cdot 10^{-1}$
b	$1.17357 \cdot 10^{-1}$
E	1

Component	Initial value
x_1	$1.44678 \cdot 10^{-2}$
x_2	$1.39604 \cdot 10^{-2}$
x_3	$1.01986 \cdot 10^{-2}$
x_4	$6.60602 \cdot 10^{-3}$
x_5	$4.57360 \cdot 10^{-3}$
x_6	$0.39604 \cdot 10^{-2}$
x_7	$0.01986 \cdot 10^{-2}$
x_8	$5.60602 \cdot 10^{-3}$
y	$2.24603 \cdot 10^{-1}$

Table 1: Parameters and Initial Values

Events We consider the follicles as being atretic if their level x_i is smaller than 0.05 for all follicles, and we reckon ovulation if $\max(x_i) > 0.99$. Whenever such an event occurs, we re-set the x_i to their initial values in Table 1, multiplied by a uniform random variable from the interval $(0, 1)$. To obtain reproducible results with MATLAB, we fix the internal state of the pseudorandom number generator with the command `rand('state',randcounter)`. The integer variable `randcounter` is increased by one every time a new follicular wave begins. The variable y is always re-set to its original initial value.

3.2 Results

Regular cycles First, we present the results for follicles, FSH, P4, and y from a simulation with 5 follicles (Figures 6(a) and 6(b)). The model generates successive estrous cycles with a length of about 22 days. As long as P4 is high, differentiation of a dominant follicle is inhibited, but ovulation takes place if P4 levels are low. Note that here and in the following, all components are dimensionless.

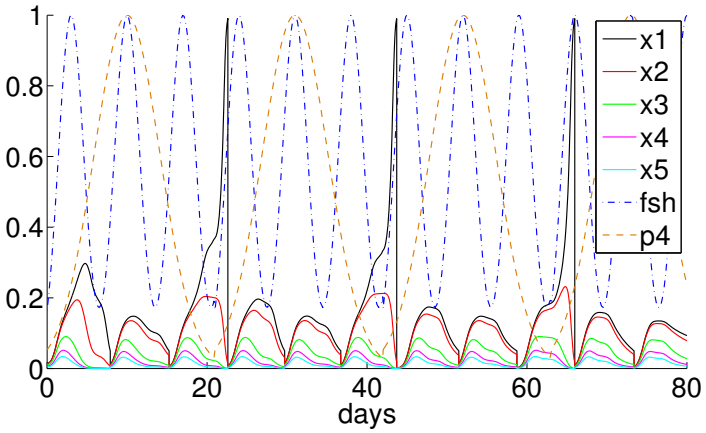

(a) Follicles, FSH, and P4

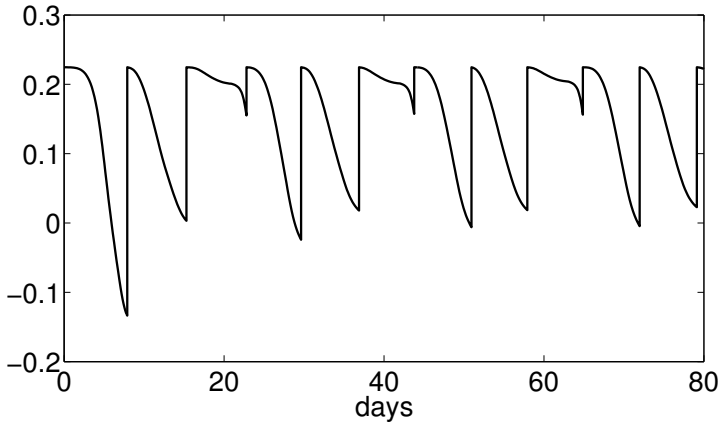

(b) $y(t)$

Figure 6: Simulation results for the new submodel: Regular estrous cycles.

Influence of the number of follicles As Figure 7 and Figure 8 show, the regular cycle pattern is maintained if we change the number of follicles.

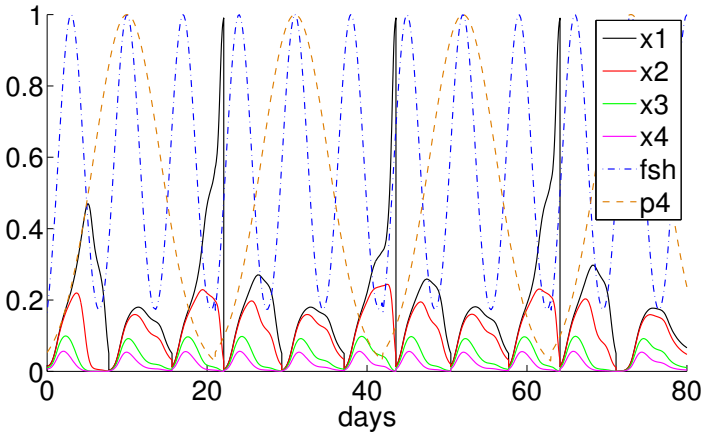

Figure 7: Simulation with 4 follicles.

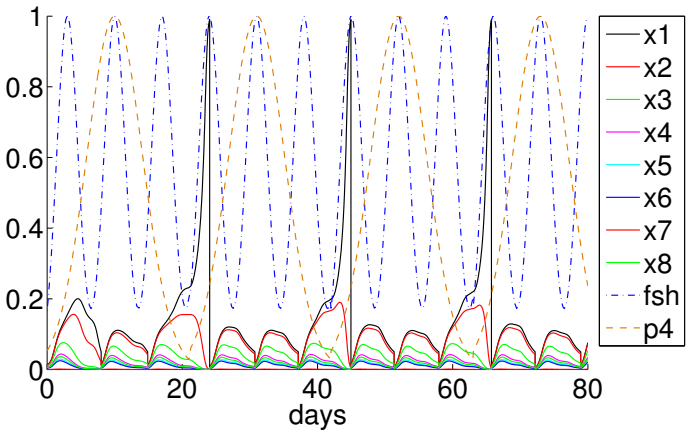

Figure 8: Simulation with 8 follicles.

Influence of initial values If we change the initial values, cycles with varying numbers of follicular waves can occur. This can also happen in reality.

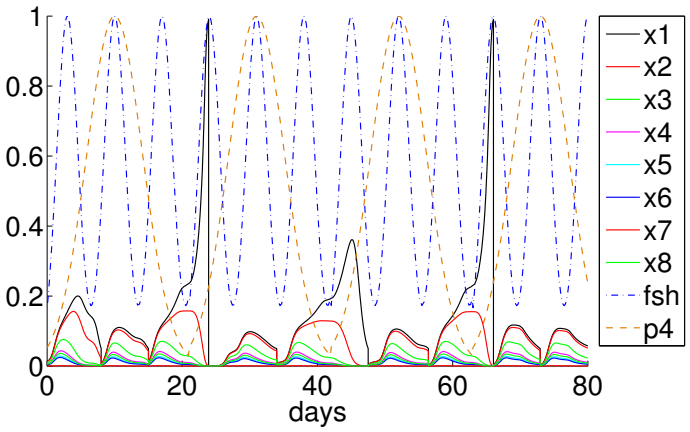

Figure 9: Simulation results for the new submodel: Estrous cycles with different numbers of follicular waves, resulting from varying initial values of the follicles.

Influence of FSH periodicity If we change the frequency of FSH, we do not obtain estrous cycles anymore, because P4 and FSH are not correctly correlated in time to promote ovulation. This example illustrates that timing is very important to obtain regular cycles.

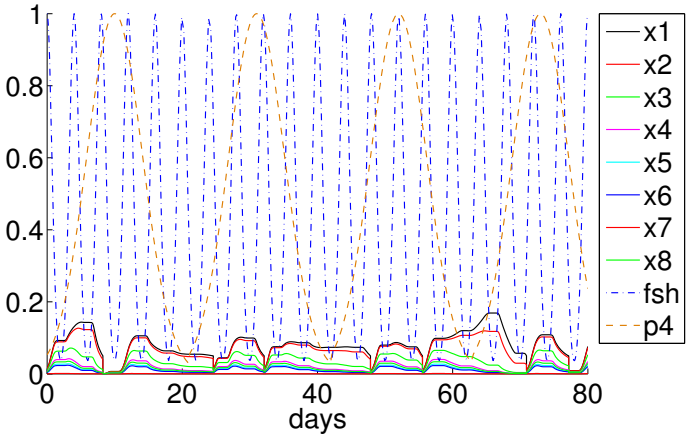

Figure 10: Higher FSH frequency results in irregular cycles.

To conclude, our sub-model is robust to changes in the initial value and in the number of follicles, but not to timing of FSH.

4 The coupled model

We now integrate the small model with multiple follicles, which was introduced in Section 3, into the large estrous cycle model that was presented in Section 2.1. In particular, FSH and P4, which played an important role in the submodel, are now the result of interactions between the hormones and no longer provided as input curves. The mechanisms of the large coupled model are depicted in Figure 11.

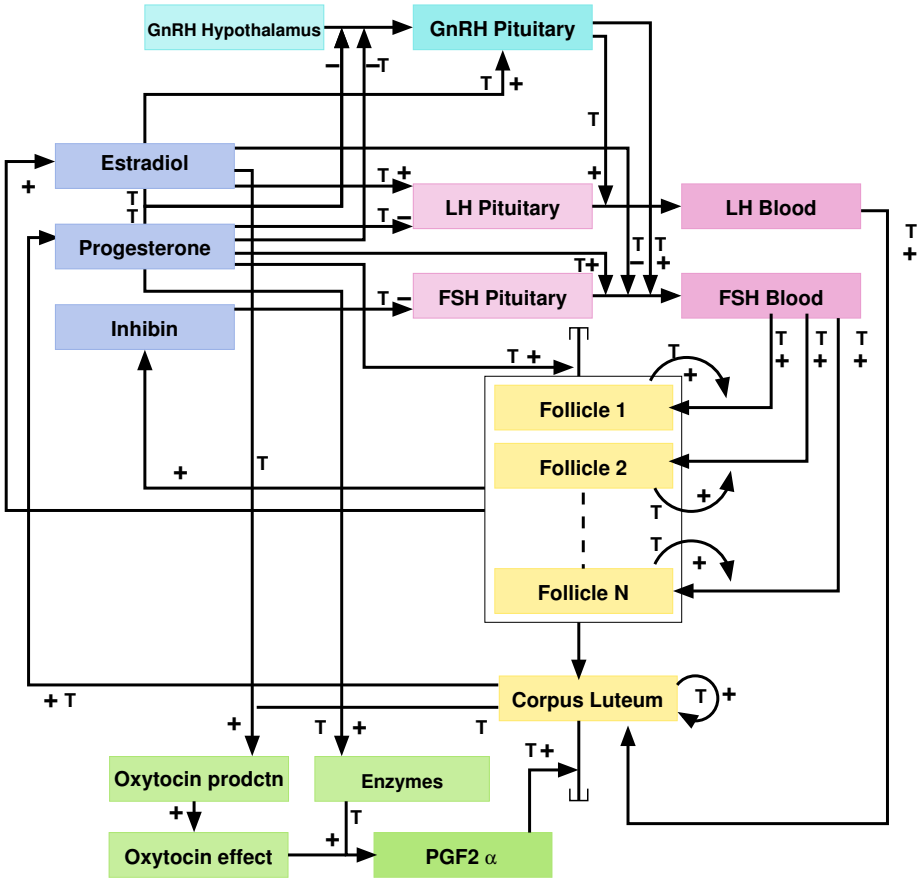

Figure 11: Schematic outline of the hormonal interactions in the fully coupled model.

4.1 Model equations

We briefly introduce the equations that have been adapted from the estrous cycle model in [18], together with the new equations from the submodel. The fully coupled model comprises 16 differential equations plus one differential equation per follicle.

The equations for follicles $i = 1, 2, \ldots, N$ are taken from the submodel in

Section 3:

$$\frac{d}{dt}x_i(t) = \frac{k \cdot \lambda^2}{E} \cdot H_{12}^{+}(FSH) \cdot x_i \cdot (E - x_i) \cdot [y - (\lambda - x_i) \cdot \sum_{j=1}^{N} x_j] \tag{12a}$$

$$\frac{d}{dt}y(t) = -a \cdot [\max(x_i) - \text{mean}(x_i)] \cdot H_{13}^{-}(P_4) \tag{12b}$$

These equations are coupled to the production of E2 and Inh in the following way:

$$\frac{d}{dt}E_2(t) = c_{x_i}^{E2} \cdot \sum_{i=1}^{N} x_i(t) - c_{E_2} \cdot E_2(t) \tag{13}$$

$$\frac{d}{dt}Inh(t) = c_{x_i}^{Inh} \cdot \sum_{i=1}^{N} x_i(t) - c_{Inh} \cdot Inh(t) \tag{14}$$

Thus, estradiol and inhibin production are directly correlated with the sum of all follicles.

The remaining equations coincide with the equations in the estrous cycle model in [18], except the following:

- LH-synthesis is bounded by a maximum capacity $LH_{\max}$.
- LH-release is additionally inhibited by P4.

$$Rel_{LH}(t) = b_{LH} \cdot H_{10}^{+}(GnRH_{Pit}) \cdot H_{11}^{-}(P_4) \cdot LH_{Pit}(t)$$

- The growth of CL is not directly initiated by LH anymore, but triggered by an event.

The detailed list of equations and parameters can be found in the appendix.

Events In the same way as in the non-coupled model, a new follicular wave begins every time the dominant follicle decays ($\max(x_i)$ reaches 0.05 from above), or reaches a size large enough for ovulation ($\max(x_i)$ reaches 0.9 from below). In both cases, the E2-sensitivity $y(t)$ is re-set to its initial value, and the follicles x_i are reassigned with new random initial values as in the submodel (Section 3). If the dominant follicle becomes larger than 0.9 *and* the LH level is higher than a certain threshold (0.2), the event is identified as ovulation. In this case, also the CL is re-set to its initial value (0.1), and a new corpus luteum starts to develop.

4.2 Results

For most of the parameters, we kept the values from the submodel and the estrous cycle model [18]. However, some parameters and initial values had to be adapted to obtain regular estrous cycles. The final list of parameter values and initial values can be found in the appendix. In the following, we present and discuss some of the simulation results. We will first consider simulations with four follicles, before we analyze the behavior of the model with respect to changes in the initial values and different numbers of follicles

4.2.1 Estrous cycle with 4 follicles

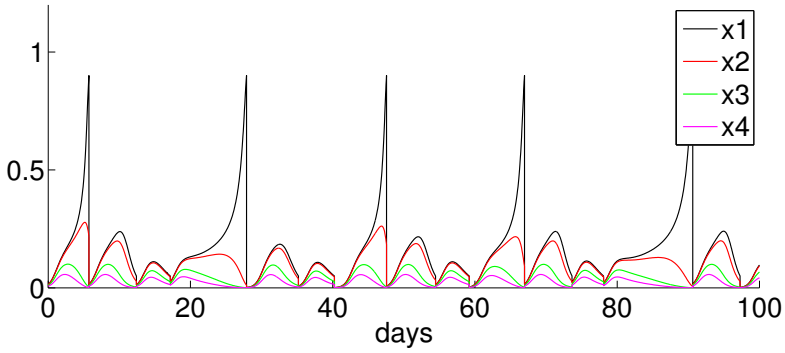

Figure 12: Follicular development in the coupled model.

Follicular waves As one can see in Figure 12, the model produces a solution with regular cycles. The cycle length varies between 18 and 24 days, and ovulation occurs in every third wave.

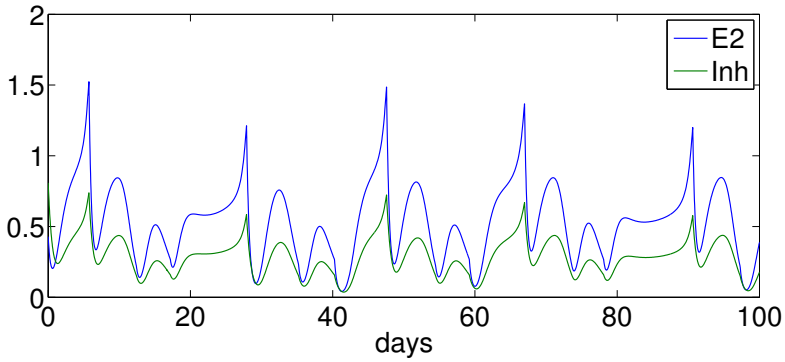

Figure 13: E2 and Inh production.

E2 and Inh production As expected from the model equations, Inh and E2 increase proportionally to the follicles (Figure 13).

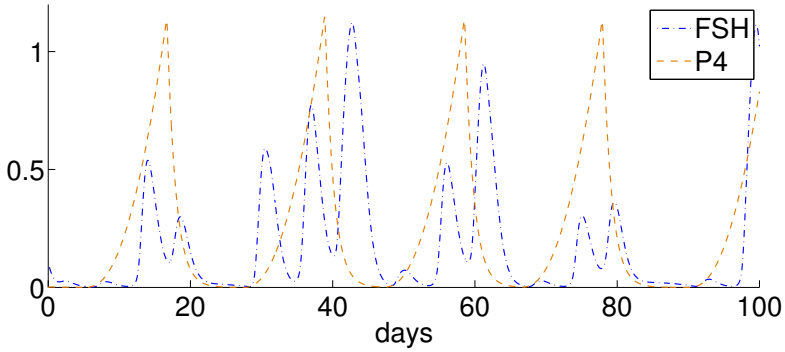

Figure 14: P4 and FSH production.

FSH and P4 The FSH and P4 levels result from interactions between the hormones and are not defined as input curves anymore. In Figure 14, it can be observed that the solutions are less smooth than in the sub-model. The influence of P4 is still significant, but now FSH levels in the first follicular wave are always very low. To maintain, nevertheless, the influence of FSH on follicular maturation, we added an artificial term 0.3 into the Hill function $H_{12}^{+}(FSH) = h^{+}(0.3 + FSH(t); T_{FSH}^{x_i}, 5)$ (Appendix B). Since this term is larger than the threshold $T_{FSH}^{x_i}$, the Hill function will always be close to one, so that it can be omitted as factor in Equation (12a). This is certainly a deficiency in the current model and needs to be improved in future work.

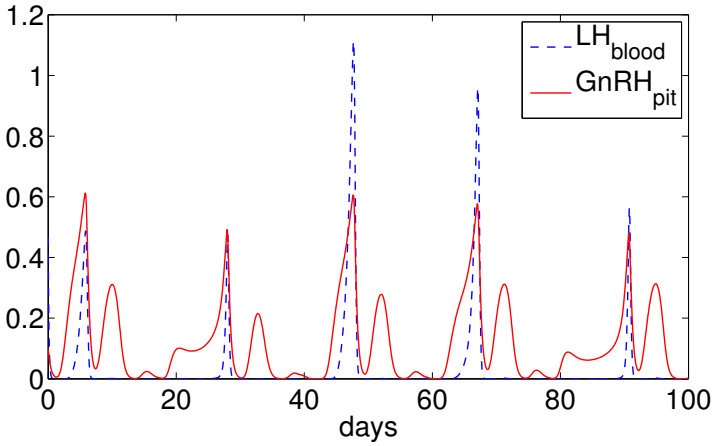

Figure 15: GnRH and LH peaks.

LH and GnRH The increase in GnRH induces the LH peak shortly before ovulation (Figure 15).

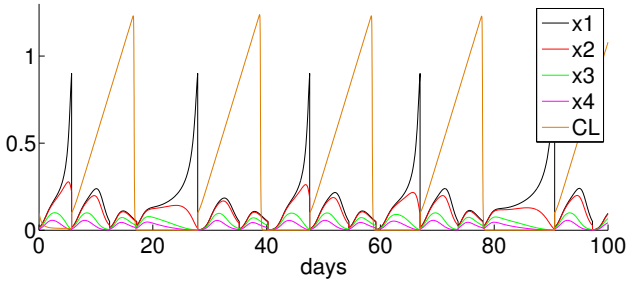

Figure 16: Growth of the corpus luteum after ovulation.

Corpus luteum The corpus luteum starts to grow right after ovulation and dies about ten days later, which might be too early compared to reality.

4.2.2 Change of initial values

It is possible to change the random initial values assigned to the follicles after each event by changing the seed of the random number generator. By simulating different cycles, we can thus evaluate the robustness of the coupled model. In fact, the model often resists changes in the initial values and shows different regular cycle patterns (Figure 17).

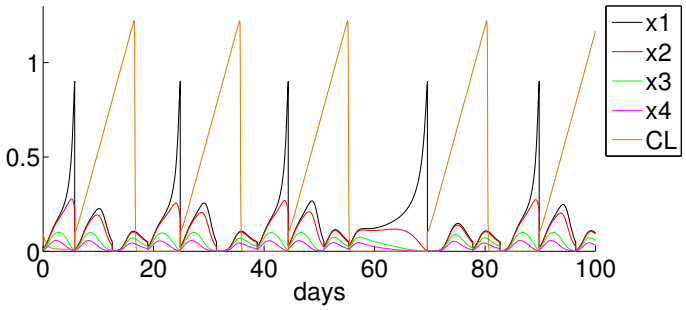

(a)

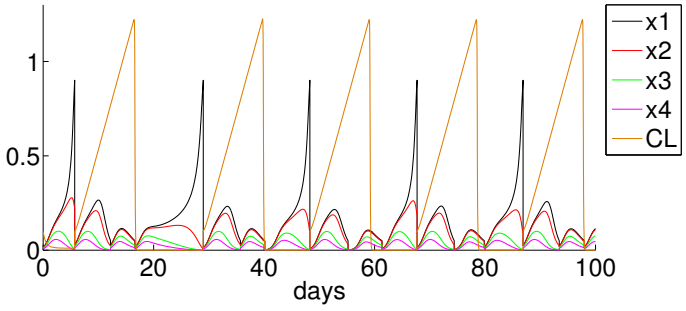

(b)

Figure 17: Follicular development in two simulations with different random initial values for the follicles.

4.2.3 Different numbers of follicles

By increasing the number of follicles, the estrous cycle becomes less regular, as one can observe in Figures 18 and 19. In case of 3 follicles, we obtain regular cycles with two follicular waves per cycle, whereas for 9 follicles sometimes 4 waves occur, sometimes ovulation is delayed by many days. It seems that the follicles become smaller if there are more of them. One might argue that the larger the number of follicles, the higher the competition between them. However, the model is certainly deficient in this point and needs improvement.

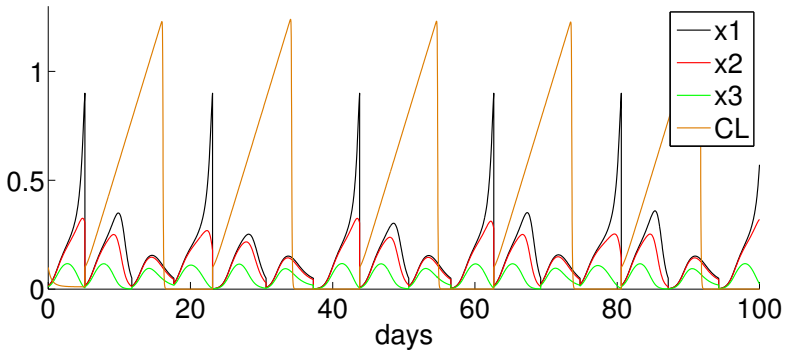

Figure 18: Simulation of the development of 3 follicles.

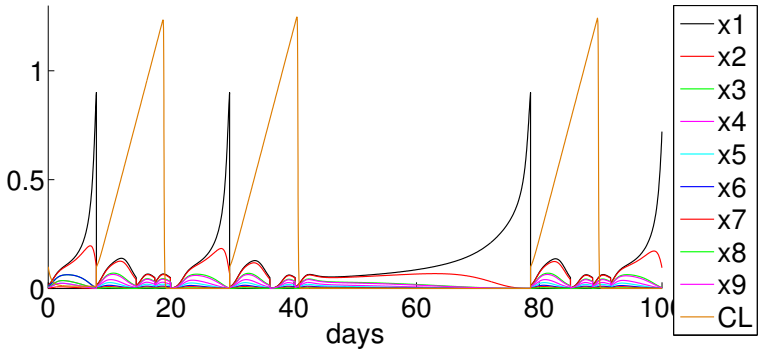

Figure 19: Simulation of the development of 9 follicles.

5 Modeling of external influences

To demonstrate the usefulness of this model and to support future expansions concerning medical requirements, it is necessary to validate the model by simulating real-world experiments.

5.1 Synchronization protocols

Estrous synchronization protocols are commonly used in cattle. They imply the successive administration of different hormones or their analogues following a precise order. Their aim is to synchronize the cycles of individual females in order to facilitate the timing of artificial insemination without considering the estrous cycle phase at the protocol beginning. However, this kind of protocol is still not entirely reliable in clinical practice.

Scientific reviews on this subject report that the protocols do not always result in the expected synchronization in all animals, though they are still able to increase the fertility rate [17]. Moreover, in many cases the factors leading to failure are not completely understood, and quantitative measures are missing. Mathematical models might help in improving and predicting the outcome of synchronization protocols.

5.1.1 Prostaglandin administration

In veterinary medicine, $PGF2\alpha$ and its analogues, PGF_{syn}, are administered mainly to make use of their luteolytic action. Thus they play an important role in synchronization protocols. The treatment effect depends on the estrous stage which determines the CL's receptivity for PGF_{syn}. Within a few days after ovulation, PGF_{syn} administration does not lead to luteolysis. Thereafter, a sudden rise of PGF_{syn} results in an immediate decay of the CL and a decrease of P4 plasma levels. We will demonstrate in the following that our model nicely captures this behavior, thus reproducing the results from [18].

To model the administration of PGF_{syn}, we use the same formalism as in [18]:

$$\frac{d}{dt}PGF_{syn}(t) = D \cdot \beta^2 \cdot t_{mod}(t) \cdot \exp(-\beta \cdot t_{mod}(t)) - c_{PGF_{syn}} \cdot PGF_{syn}(t) \quad (15)$$

The parameter D represents the amount of drug, scaled to obtain the designated height of the relative level of PGF_{syn}. The parameter $c_{PGF_{syn}}$ denotes the clearance rate constant of PGF_{syn}. The modified time function t_{mod} is given as:

$$t_{mod}(t) = \max(0, t - t_D)$$

The rise of PGF_{syn} is large right after dosing time and approaches zero quickly thereafter, leading to a rapid decay of the function (Figure 20).

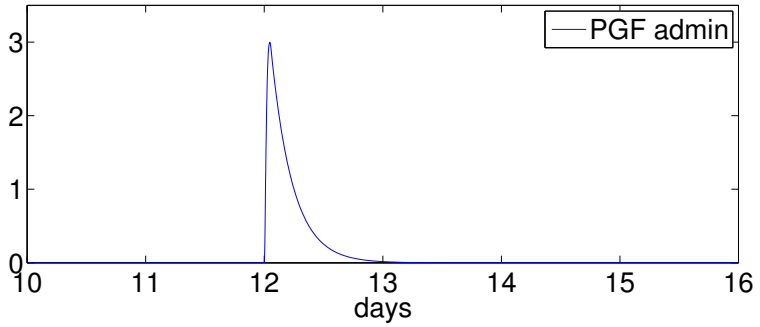

Figure 20: Administration of PGF_{syn} at time $t_D = 12$ (D = 3.7, $\beta = 100$, $c_{PGF_{syn}} = 5.5$).

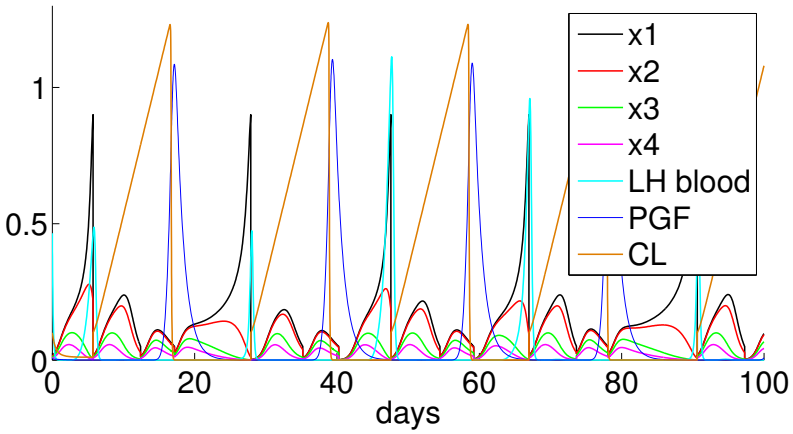

Figure 21: Visualization of the cycle without treatment.

We will now consider the influence of PGF_{syn} on the cycle. For this purpose, the action of $PGF2\alpha$ in the model equations is replaced by $PGF2\alpha + PGF_{syn}$. Figure 21 shows the estrous cycle without artificial administration of PGF_{syn}. PGF_{syn} administration right after ovulation slightly delays the first wave, but does not have an influence on the next ovulation (Figure 22). Administration 4 days after ovulation (Figure 23) results in a next ovulation within the same wave six days later. If administration takes place when the follicles are decaying, ovulation does not occur until the next wave (Figure 24).

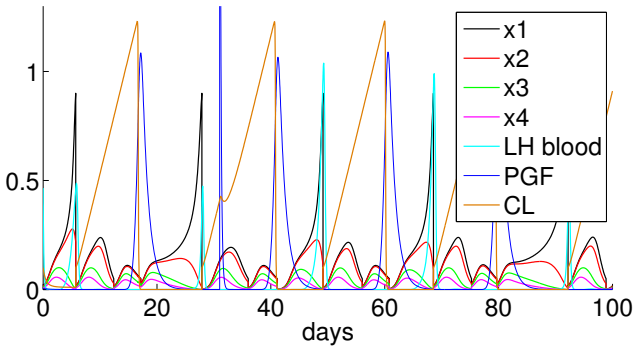

Figure 22: Administration of PGF_{syn} 3 days after ovulation slightly delays the cycle, but has no effect on ovulation.

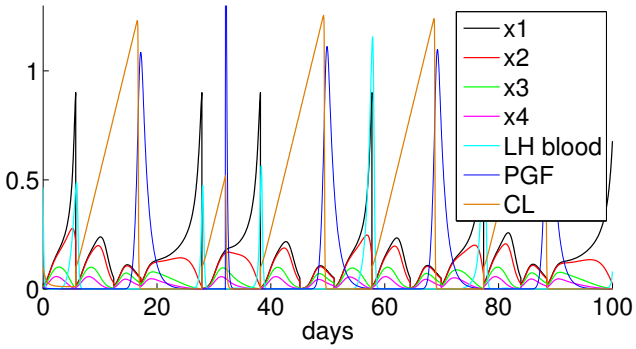

Figure 23: Administration of PGF_{syn} 4 days after ovulation results in ovulation in the first wave.

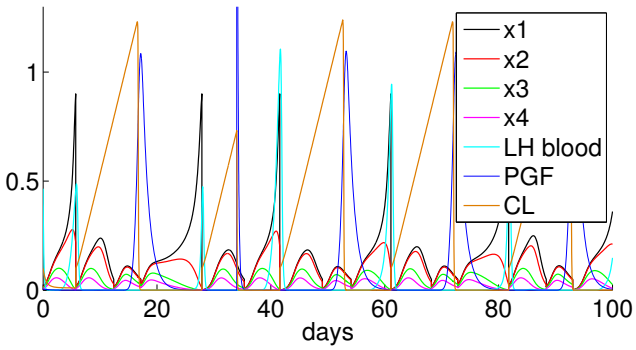

Figure 24: Administration of PGF_{syn} 6 days after ovulation leads to ovulation in the second wave.

5.1.2 Combined therapies

We have tested the influence of continuous P4 administration during a couple of days, followed by a single administration of PGF_{syn} as described in [17]. For the protocol being effective in our simulations, we reduced the P4 administration from seven days [17] to five days. This requirement might be due to the short life-span of the corpus luteum.

It is in fact a combination of GnRH, PGF_{syn} and P4, that is used in [17], since GnRH administration at the beginning of the protocol is reported to increase the ovulation rate. In our model, however, this administration does not have any influence. The administration of GnRH is therefore omitted in the following.

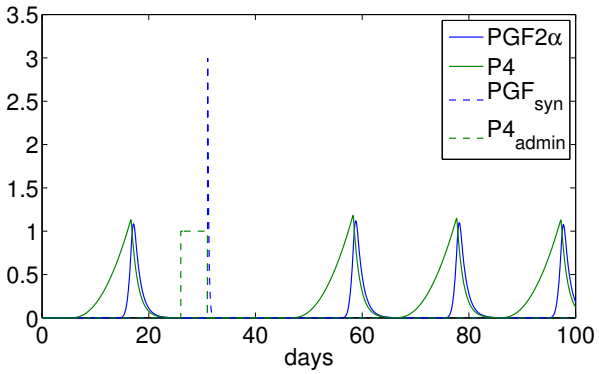

Figure 25: Visualization of the protocol for days 26 to 31.

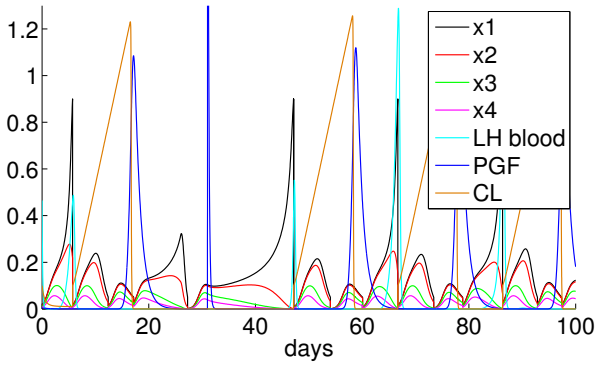

Figure 26: Effect of the protocol on days 26 to 31.

As shown in Figure 25, the simulated protocol consists of a continuous administration of P4 followed by a single injection of PGF_{syn}. This protocol was applied at different stages of the cycle. In a first experiment, P4 administration starts shortly before ovulation (Figure 26). This administration prevents ovulation. Finally, PGF_{syn} administration at the end of the protocol causes ovulation not until day 470 because follicular development is very slow. However, as stated in [17], the protocol does not always lead to ovulation on the

desired day.

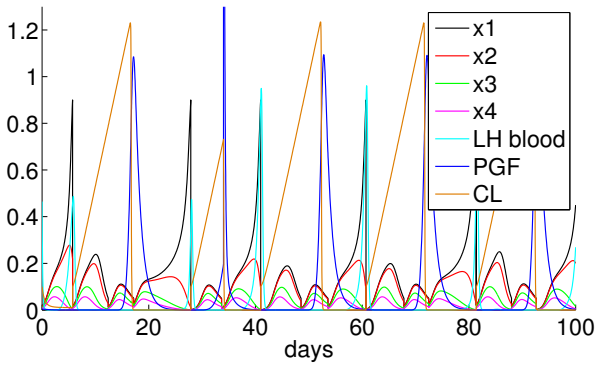

(a) Standard protocol on days 29 to 34.

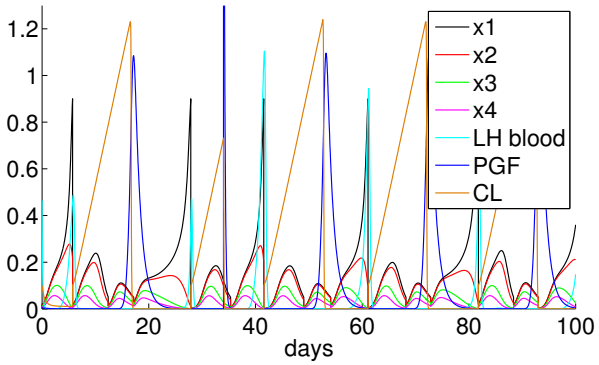

(b) Administration of PGF_{syn} on day 34.

Figure 27: Comparison between the standard protocol (5 days P4 plus a single dose PGF_{syn}) and a single dose PGF_{syn} without preceding P4 treatment.

We now compare the influence of P4 administration between days 29 and 34 before PGF_{syn} administration, with the single administration of PGF_{syn} on day 34 without preceding P4 treatment. Figure 27(a) shows the simulation with P4 administration. At P4 removal, a new wave begins which leads to ovulation on day 41. Without this P4 administration (Figure 27(b)), ovulation occurs one day later. Compared to the standard protocol, one can observe around day 33 that the follicles are larger if P4 is not administered.

If administered during the last follicular wave of a cycle (Figures 28 and 29), P4 inhibits the growth of the follicles and thus ovulation. Therefore the cycle counts three waves before the ovulating wave. Depending on the timing of the protocol, it might also happen that ovulation is delayed by some weeks (Figure 29).

To conclude, P4 administration inhibits the maturation of follicles and prevents ovulation during the treatment period. PGF_{syn} causes the decay of the corpus luteum, and the following follicular wave will lead to ovulation.

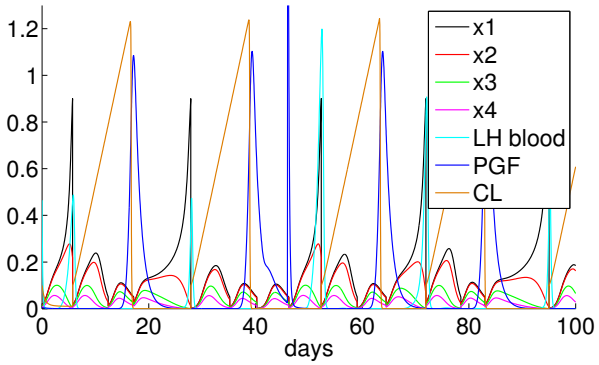

Figure 28: Effect of the standard protocol on days 41 to 46.

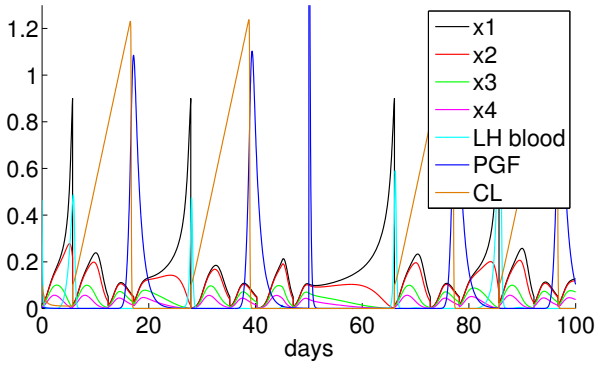

Figure 29: Effect of the standard protocol on days 45 to 50.

5.2 Postpartum anestrus

Dairy cows are pregnant most of the lactation period. Pregnancy and lactation are accompanied by marked cardiovascular end endocrine adaptations. A negative energy balance during early lactation in dairy cows can lead to metabolic dysfunctions such as infertility. If estrus has not been observed in a dairy cow by 60 days post partum the condition is defined as Post Partum Anestrus (PPA).

Recovery of cyclicity after calving is influenced by body condition score at calving and nutritional status during early lactation [13]. Insulin is an important hormone in this process. It controls the pulsatile secretion of LH and increases the sensitivity of the ovary to this gonadotropin [13]. Low insulin levels promote a long anestrus period.

To observe this effect in our model, we have to change parameter values and initial values in such a way that LH frequency is low at the beginning of the simulation, and slowly increases until the first ovulation. LH frequency can be reduced by lowering the amount of GnRH in the pituitary, which can again be achieved by reducing GnRH frequency.

5.2.1 Change of model parameters

In order to model the post partum anestrus, we decreased the basal GnRH frequency from 1/day to

$$b_{GnRH} := 0.003/\text{day}.$$

Since this reduces the release from the hypothalamus, we increased the maximum capacity from $16 \cdot [GnRH_{Hypo}]$ to

$$GnRH_{Hypo}^{\max} := 32 \cdot [GnRH_{Hypo}].$$

Finally, in order to stimulate the LH frequency even if the GnRH concentration is smaller we decrease the threshold T_{GnRH}^{LH} from $0.69 \cdot [GnRH]$ to

$$T_{GnRH}^{LH} = 0.1 \cdot [GnRH].$$

Keeping all other parameter values and initial values unchanged, we can observe anestrus for a period of about 40 days at the beginning of the simulation (Figure 30). Even though a dominant follicle develops in every wave, the level of LH at the beginning of the simulation is too low to cause ovulation (Figure 31). This is due to lowered levels of GnRH in the hypothalamus (Figure 32) and the pituitary. However, the solution equilibrates within about 40 days and returns to the quasi-periodic "normal" cycle for the remaining time.

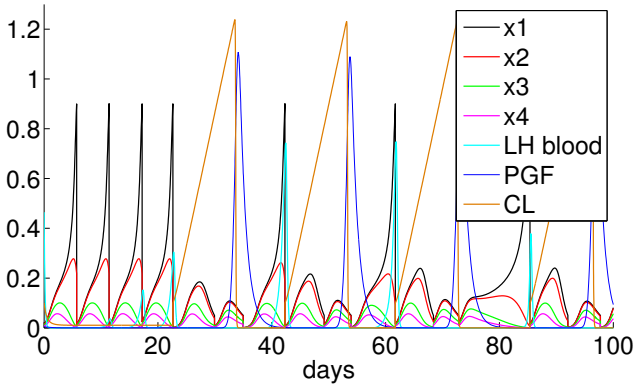

Figure 30: Follicles during anovulatory and ovulatory cycles.

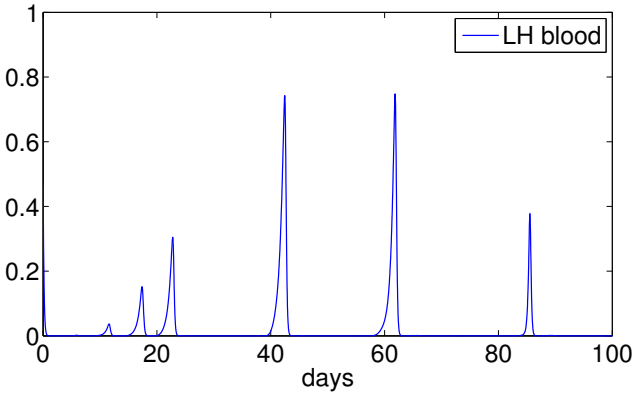

Figure 31: LH blood level during anovulatory and ovulatory cycles.

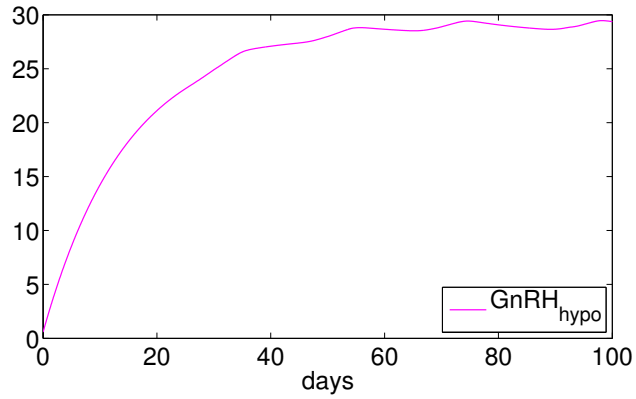

Figure 32: GnRH level in the hypothalamus during anovulatory and ovulatory cycles.

5.2.2 Change of initial values

The change of parameters in the previous section is still biologically reasonable since the solution equilibrates towards regular cycles. To obtain such regular cycles already at the beginning of the simulation, we need to change the initial values. Except for the follicles and the variable $y(t)$, we select values from the previous simulation at some point in time when the cycle already recovered to a regular pattern. These values are listed in Table 2. They could be interpreted as the state of a healthy cow, whereas the previous values correspond to a cow after gestation.

Component	Initial value
$GnRH_{Hypo}$	$2.90479 \cdot 10^{+1}$
$GnRH_{Pit}$	$2 \cdot 10^{-4}$
FSH_{Pit}	$6.972 \cdot 10^{-1}$
FSH_{Blood}	$2.439 \cdot 10^{-1}$
LH_{Pit}	$3.3479 \cdot 10^{+1}$
LH_{Blood}	0
E_2	$3.347 \cdot 10^{-1}$
$PGF2\alpha$	0
CL	$8.839 \cdot 10^{-1}$
P_4	$5.287 \cdot 10^{-1}$
Inh	$1.654 \cdot 10^{-1}$
Enz	$9.79 \cdot 10^{-2}$
OT	1.1385
IO	$1.55 \cdot 10^{-2}$

Table 2: Initial values leading to regular estrous cycles.

As expected, these changes lead to regular cycles right from the beginning (Figure 33). However, these changes have not been validated due to the lack of empirical data.

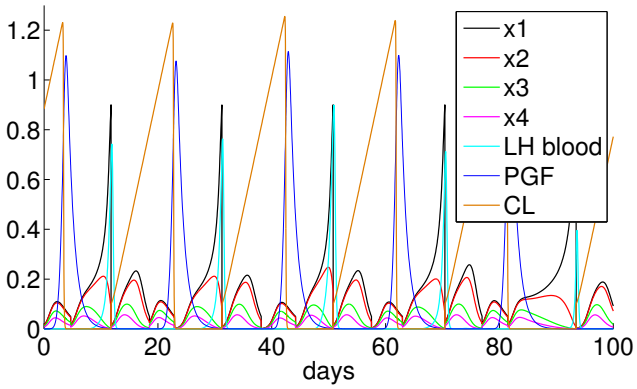

Figure 33: Estrous cycles without post partum anestrus.

Conclusion

This work continues a series of previous modeling activities on the bovine estrous cycle. Thanks to the robustness of the large estrous cycle model by Stötzel et al. [18], it can easily be coupled with other models. In the study presented here we have extended the model by including multiple follicles. The new model can generate regular estrous cycles with multiple follicular waves per cycle, as well as anovulatory waves by changing certain parameters and initial values. In addition, the model correctly predicts the effect of prostaglandin administration on ovulation. However, there are still some deficiencies. For example, the influence of the gonadotropins on follicular development is still not modeled satisfactory. LH determines at least the timepoint of ovulation, whereas FSH has nearly no influence on follicular maturation. This needs to be improved in future work. Moreover, several studies indicate that consecutive follicular waves are not separated, but that they overlay each other [2, 7]. This feature is not yet captured by the model. Besides, the model could be refined by including the influence of other hormones, e.g. insulin, which has a large impact on LH frequency. Nevertheless, we hope that the model presented here will serve as a starting point for other researchers in this area. In particular, we intend to validate the model with experimental data.

Acknowledgment

The authors would like to thank Claudia Stötzel for providing her latest results on the bovine estrous cycle model and for her helpful comments on the manuscript.

A Equations of the coupled model

In this part we list all equations that have been used and adapted from the estrous cycle model in [18], together with our new equations. The complete model comprises 16 differential equations plus one differential equation per follicle.

Equation of GnRH The amount of GnRH in the hypothalamus is a result of synthesis in the hypothalamus and release into the pituitary,

$$\frac{d}{dt} GnRH_{Hypo}(t) = Syn_{GnRH}(t) - Rel_{GnRH}(t). \tag{A.1}$$

GnRH synthesis depends on its current level in the hypothalamus. If this level approaches a specified threshold, synthesis decreases until zero. This effect is modeled as logistic growth,

$$Syn_{GnRH}(t) = c_{GnRH,1} \cdot \left(1.0 - \frac{GnRH_{Hypo}(t)}{GnRH_{Hypo}^{\max}}\right). \tag{A.2a}$$

As long as GnRH is far below its maximum, the factor $1 - \frac{GnRH_{Hypo}(t)}{GnRH_{Hypo}^{\max}}$ has only a small impact. The release of GnRH from the hypothalamus to the pituitary depends on its current level in the hypothalamus and the frequency. E2 inhibits GnRH frequency during the luteal phase, i.e. if P4 and E2 are high at the same time during the luteal phase. This is described by $H_1^-(P_4\&E_2)$. Additionally, the release of GnRH is inhibited by P4 only.

$$Rel_{GnRH}(t) = Freq_{GnRH} \cdot GnRH_{Hypo}(t) \tag{A.2b}$$

$$Freq_{GnRH} = b_{GnRH} \cdot (H_1^-(P_4\&E_2) + H_2^-(P_4)) \tag{A.2c}$$

Changes in GnRH levels in the pituitary are dependent on the released amount from the hypothalamus, but also on the presence of E2. E2 increases the number of GnRH receptors in the pituitary. This effect is included in the equation as a positive Hill function. GnRH clearance from pituitary portal blood is proportional to the GnRH level in the pituitary, i.e. GnRH clearance is represented by $c_{GnRH,2} \cdot GnRH_{Pit}(t)$, in which $c_{GnRH,2}$ is a constant,

$$\frac{d}{dt} GnRH_{Pit}(t) = Rel_{GnRH}(t) \cdot H_3^+(E_2) - c_{GnRH,2} \cdot GnRH_{Pit}(t). \tag{A.2}$$

Equation of FSH FSH is synthesized in the pituitary and released into the blood,

$$\frac{d}{dt} FSH_{Pit}(t) = Syn_{FSH}(t) - Rel_{FSH}(t). \tag{A.3}$$

FSH synthesis rate in the pituitary is only dependent on inhibin, as in [8]. FSH is synthesized when the Inh level is low, i.e. high Inh levels inhibit FSH synthesis, which is included as a negative Hill function,

$$Syn_{FSH} = H_4^-(Inh). \tag{A.4a}$$

FSH release from the pituitary to the blood is stimulated by P4 and GnRH, and inhibited by E2,

$$Rel_{FSH} = (b_{FSH} + H_5^+(P_4) + H_6^-(E_2) + H_7^+(GnRH_{Pit})) \cdot FSH_{Pit}(t). \tag{A.4b}$$

Concluding, FSH serum level is a result of the difference between the released amount from the pituitary and clearance from the blood,

$$\frac{d}{dt}FSH_{Blood}(t) = Rel_{FSH}(t) - c_{FSH} \cdot FSH_{Blood}(t), \tag{A.4}$$

where c_{FSH} is the FSH clearance rate constant.

Equation of LH Like FSH, the LH serum level depends on synthesis in the pituitary, release into the blood and clearance thereof,

$$\frac{d}{dt}LH_{Pit}(t) = Syn_{LH}(t) - Rel_{LH}(t). \tag{A.5}$$

LH synthesis in the pituitary is stimulated by E2 and inhibited by P4,

$$Syn_{LH}(t) = (H_8^+(E_2) + H_9^-(P_4)) \cdot \left(1.0 - \frac{LH(t)}{LH_{\max}}\right) \tag{A.6a}$$

Synthesis stops if a maximum capacity $LH_{\max}$ is reached. LH release depends on the frequency, which is stimulated by GnRH and inhibited by P4.

$$Rel_{LH}(t) = Freq_{LH} \cdot LH_{Pit}(t) \tag{A.6b}$$

$$Freq_{LH} = b_{LH} \cdot H_{10}^+(GnRH_{Pit}) \cdot H_{11}^-(P_4) \tag{A.6c}$$

Summarizing, LH in the blood is obtained as

$$\frac{d}{dt}LH_{Blood}(t) = Rel_{LH}(t) - c_{LH} \cdot LH_{Blood}(t), \tag{A.6}$$

where c_{LH} is the LH clearance rate constant.

Equations of follicular development Maturation of the i-th follicle is modeled as

$$\frac{d}{dt}x_i(t) = \frac{k \cdot \lambda^2}{E} \cdot H_{12}^+(FSH) \cdot x_i \cdot (E - x_i) \cdot [y - (\lambda - x_i) \cdot \sum_{j=1}^{N} x_j,] \tag{A.7}$$

$$\frac{d}{dt}y(t) = -a \cdot [\max(x_i) - \text{mean}(x_i)] \cdot H_{13}^-(P_4). \tag{A.8}$$

Equation of CL The CL development depends on three mechanisms : an initiating impulse from an ovulating follicle, a self-growth, and the decay due to the inter-ovarian factor (IOF). CL changes as follows in the model : At the time of ovulation, CL is re-set to an initial size T_{CL}^{CL} sufficient for self-growth. Then it grows until the rise of PGF2α and thus in IOF induces its decay.

$$\frac{d}{dt}IOF(t) = H_{18}^+(PGF2\alpha) \cdot H_{19}^+(CL) - c_{IOF} \cdot IOF(t) \tag{A.9}$$

$$\frac{d}{dt}CL(t) = H_{20}^+(CL) - H_{21}^+(IOF) \cdot CL(t) \tag{A.10}$$

Equations of P4, E2, and Inh The rise of P4 depends quadratically on CL to obtain lower P4 levels at the beginning of CL growth compared to later luteal stages [18]. The production of E2 and Inh is assumed to be proportional to follicular function.

$$\frac{d}{dt}P_4(t) = c_{CL}^{P_4} \cdot CL(t)^2 - c_{P_4} \cdot P_4(t) \tag{A.11}$$

$$\frac{d}{dt}E_2(t) = c_{x_i}^{E2} \cdot \sum_{i=1}^{N} x_i(t) - c_{E_2} \cdot E_2(t) \tag{A.12}$$

$$\frac{d}{dt}Inh(t) = c_{x_i}^{Inh} \cdot \sum_{i=1}^{N} x_i(t) - c_{Inh} \cdot Inh(t) \tag{A.13}$$

The parameters c_{P_4}, c_{E_2} and c_{Inh} denote the respective clearance rate constants.

Equation of PGF2α PGF2α initiates the functional regression of the CL, and thereby the decrease in P4 levels. P4 has a stimulating effect on the enzyme production, E2 activates oxytocin (OT) synthesis in the granulosa cells, and OT initiates PGF2α peaks.

$$\frac{d}{dt}Enz(t) = H_{14}^{+}(P_4) - c_{Enz} \cdot Enz(t) \tag{A.14}$$

$$\frac{d}{dt}OT(t) = H_{15}^{+}(E_2) \cdot CL(t)^2 - c_{OT} \cdot OT(t) \tag{A.15}$$

$$\frac{d}{dt}PGF2\alpha(t) = H_{16}^{+}(Enz) \cdot H_{17}^{+}(OT) - c_{PGF2\alpha} \cdot PGF2\alpha(t) \tag{A.16}$$

Detailed notations for the Hill functions and parameters are given in Appendices B and C, respectively.

B List of Hill functions

$$
\begin{aligned}
H_1^-(P4\&E2) &:= m_{P4\&E2} \cdot \Big(h^-(P4(t); T_{P4}^{GnRH,1}, 2) + h^-(E2(t), T_{E2}^{GnRH,1}, 2) \\
&\qquad - h^-(P4(t); T_{P4}^{GnRH,1}, 2) \cdot h^-(E2(t), T_{E2}^{GnRH,1}, 2)\Big) \\
H_2^-(P4) &:= m_{P4}^{GnRH,2} \cdot h^-(P4(t), T_{P4}^{GnRH,2}, 2) \\
H_3^+(E2) &:= m_{E2}^{GnRH,2} \cdot h^+(E2(t), T_{E2}^{GnRH,2}, 5) \\
H_4^-(Inh) &:= m_{Inh}^{FSH} \cdot h^-(Inh(t), T_{Inh}^{FSH}, 5) \\
H_5^+(P4) &:= m_{P4}^{FSH} \cdot h^+(P4(t); T_{P4}^{FSH}, 2) \\
H_6^-(E2) &:= m_{E2}^{FSH} \cdot h^-(E2(t); T_{E2}^{FSH}, 2) \\
H_7^+(GnRH_{Pit}) &:= m_{GnRH}^{FSH} \cdot h^+(GnRH_{Pit}(t); T_{GnRH}^{FSH}, 1) \\
H_8^+(E2) &:= m_{E2}^{LH} \cdot h^+(E2(t); T_{E2}^{LH}, 2) \\
H_9^-(P4) &:= m_{P4}^{LH} \cdot h^-(P4(t); T_{P4}^{LH}, 2) \\
H_{10}^+(GnRH_{Pit}) &:= m_{GnRH}^{LH} \cdot h^+(GnRH_{Pit}(t); T_{GnRH}^{LH}, 5) \\
H_{11}^-(P4) &:= m_{P4}^{freq} \cdot h^-(P4(t); T_{P4}^{LH}(t), 2), \\
H_{12}^+(FSH) &:= h^+(0.3 + FSH(t); T_{FSH}^{x_i}, 5) \\
H_{13}^-(P4) &:= h^-(P4(t); T_{P4}^{x_i}, 2) \\
H_{14}^+(P4) &:= m_{P4}^{Enz} \cdot h^+(P4(t); T_{P4}^{Enz}, 5) \\
H_{15}^+(E2) &:= m_{E2}^{OT} \cdot h^+(Enz(t); T_{E2}^{OT}, 2) \\
H_{16}^+(Enz) &:= m_{Enz}^{PGF2\alpha} \cdot h^+(Enz(t), T_{Enz}^{PGF2\alpha}, 5) \\
H_{17}^+(OT) &:= m_{OT}^{PGF2\alpha} \cdot h^+(OT(t); T_{OT}^{PGF2\alpha}, 2) \\
H_{18}^+(PGF2\alpha) &:= m_{PGF2\alpha}^{IOF} \cdot h^+(PGF2\alpha(t); T_{PGF2\alpha}^{IOF}, 5) \\
H_{19}^+(CL) &:= m_{CL}^{IOF} \cdot h^+(CL(t); T_{CL}^{IOF}, 10) \\
H_{20}^+(CL) &:= m_{CL}^{CL} \cdot h^+(CL(t); T_{CL}^{CL}, 5) \\
H_{21}^+(IOF) &:= m_{IOF}^{CL} \cdot h^+(IOF(t); T_{IOF}^{CL}, 5)
\end{aligned}
$$

C List of parameters and initial values

Component	Initial value
$GnRH_{Hypo}$	$5.807 \cdot 10^{-1}$
$GnRH_{Pit}$	$8.828 \cdot 10^{-1}$
FSH_{Pit}	$5.33 \cdot 10^{-2}$
FSH_{Blood}	$1.072 \cdot 10^{-1}$
LH_{Pit}	2.2868
LH_{Blood}	$4.651 \cdot 10^{-1}$
E_2	$4.290 \cdot 10^{-1}$
$PGF2\alpha$	$5.06 \cdot 10^{-3}$
CL	$6.51 \cdot 10^{-2}$
P_4	$4 \cdot 10^{-4}$
Inh	$8.084 \cdot 10^{-1}$
Enz	$3.508 \cdot 10^{-1}$
OT	$1.83 \cdot 10^{-2}$
IO	$2.53 \cdot 10^{-1}$
y	$2.24603 \cdot 10^{-1}$
x_1	$1.44678 \cdot 10^{-2}$
x_2	$1.39604 \cdot 10^{-2}$
x_3	$1.01986 \cdot 10^{-2}$
x_4	$6.60602 \cdot 10^{-3}$
x_5	$4.57360 \cdot 10^{-3}$
x_6	$1.01986 \cdot 10^{-2}$
x_7	$1.57360 \cdot 10^{-3}$
x_8	$6.60602 \cdot 10^{-3}$
x_9	$4.57360 \cdot 10^{-3}$

Table 3: Initial Values

Table 4: List of parameters. [·] denotes the physical unit. In the present model, the time unit [t] is equal to days.

Parameter	Value	Unit
$GnRH_{Hypo}^{\max}$	1.6e+1	$[GnRH_{Hypo}]$
$c_{GnRH,1}$	1.925	$[GnRH_{Hypo}]/[t]$
b_{GnRH}	1	$1/[\mathrm{t}]$
$m_{P_4\&E_2}$	1.435	–
$T_{E_2}^{GnRH,1}$	9.72e-2	$[E2]$
$T_{P_4}^{GnRH,1}$	3.5e-1	$[P4]$
$m_{P_4}^{GnRH,2}$	1.337	–
$T_{P_4}^{GnRH,2}$	2.52e-1	$[P4]$
$m_{E_2}^{GnRH,2}$	9.9e-1	$[GnRH_{Pit}]/[GnRH_{Hypo}]$
$T_{E_2}^{GnRH,2}$	8.48e-1	$[E2]$
$c_{GnRH,2}$	2.6297	$1/[t]$
m_{Inh}^{FSH}	2.947	$[FSH]/[t]$
T_{Inh}^{FSH}	1.18e-1	$[Inh]$
b_{FSH}	6.636e-1	$1/[t]$
$m_{P_4}^{FSH}$	2.051e-1	$1/[t]$
$T_{P_4}^{FSH}$	1.52e-1	$[P4]$
$m_{E_2}^{FSH}$	2.772e-1	$1/[t]$
$T_{E_2}^{FSH}$	3.12e-1	$[E2]$
m_{GnRH}^{FSH}	1.211	$1/[t]$
T_{GnRH}^{FSH}	7.08e-2	$[GnRH]$
c_{FSH}	1.911	$1/[t]$
$m_{E_2}^{LH}$	1	$[LH]/[t]$
$T_{E_2}^{LH}$	2.43e-1	$[E2]$
$m_{P_4}^{LH}$	1.897	$[LH]$
$T_{P_4}^{LH}$	2.69e-2	$[P4]$
$LH_{\max}$	5e+1	$[LH]$
m_{GnRH}^{LH}	2.22	–
T_{GnRH}^{LH}	6.9e-1	$[GnRH]$
$m_{P_4}^{freq}$	1.897	–
b_{LH}	2.464e-1	$1/[t]$
c_{LH}	8.4	$1/[t]$
k	3.136e+1	$1/(t \cdot [x_i]^4)$
λ	5.476e-1	$[x_i]$
E	1	$[x_i]$
$T_{FSH}^{x_i}$	2.5e-1	$[FSH]$
a	2.492	$[x_i]/[t]$
$T_{P_4}^{x_i}$	5.868e-2	$[P4]$
$T_{OT}^{PGF2\alpha}$	3	$[OT]$
$m_{Enz}^{PGF2\alpha}$	3.774e+1	$[PGF2\alpha]/[t]$
$T_{Enz}^{PGF2\alpha}$	1.43	$[Enz]$
$c_{PGF2\alpha}$	8.61e-1	$[t]$

Continued on next page...

Table 4 – *continued from previous page*

Parameter	Value	Unit
$m_{P_4}^{Enz}$	2.506	$[Enz]/[t]$
$T_{P_4}^{Enz}$	7.7e-1	$[P4]$
c_{Enz}	2.086	$1/[t]$
$m_{E_2}^{OT}$	1.113	$[OT]/([CL]^2 \cdot [t])$
$T_{E_2}^{OT}$	1.43e-1	$[E2]$
c_{OT}	4.508e-1	$1/[t]$
m_{CL}^{CL}	1.071e-1	$[CL]/[t]$
T_{CL}^{CL}	1e-1	$[CL]$
m_{IOF}^{CL}	2.573e+1	$[CL]/[t]$
T_{IOF}^{CL}	4e-1	$[IOF]$
$m_{PGF2\alpha}^{IOF}$	2.778e+1	$[t]$
$T_{PGF2\alpha}^{IOF}$	1.22	$[PGF2\alpha]$
T_{CL}^{IOF}	6e-1	$[CL]$
c_{IOF}	2.086e-1	$1/[t]$
c_{CL}^{P4}	7.416e-1	$[P4]/([CL] \cdot [t])$
c_{P_4}	8.197e-1	$1/[\mathrm{t}]$
$c_{x_i}^{E_2}$	4.145	$[E2]/([x_i] \cdot [t])$
c_{E_2}	2.593	$1/[\mathrm{t}]$
$c_{x_i}^{Inh}$	1.323	$[Inh]/([x_i] \cdot [t])$
c_{Inh}	1.568	$1/[t]$

References

[1] G.P. Adams, R. Jaiswal, J. Singh, and P. Malhi. Progress in understanding ovarian follicular dynamics in cattle. *Theriogenology*, 69:72–80, 2008.

[2] A. R. Baerwald. Human antral folliculogenesis: What we have learned from the bovine and equine models. *Anim. Reprod.*, 6(1):20–29, 2009.

[3] H.M.T. Boer, S. Röblitz, C. Stötzel, R.F. Veerkamp, B. Kemp, and H. Woelders. Mechanisms regulating follicle wave patterns in the bovine estrous cycle investigated with a mathematical model. *J. Dairy Sci.*, 94(12):5987–6000, 2011.

[4] H.M.T. Boer, C. Stötzel, S. Röblitz, P. Deuflhard, R.F. Veerkamp, and H. Woelders. A simple mathematical model of the bovine estrous cycle: follicle development and endocrine interactions. *J. Theoret. Biol.*, 278(1):20–31, 2011.

[5] L. M. Chagas, J. J. Bass, D. Blache, C. R. Burke, J. K. Kay, D. R. Lindsay, M. C. Lucy, G. B. Martin, S. Meier, F. M. Rhodes, J. R. Roche, W. W. Thatcher, and R. Webb. New perspectives on the roles of nutrition and metabolic priorities in the subfertility of high-producing dairy cows. *J. Dairy Sci.*, 90:4022–4032, 2007.

[6] F. Clément, D. Monniaux, J.-C. Thalabard, and D. Claude. Contribution of a mathematical modelling approach to the understanding of the ovarian function. *C. R. Biol.*, 325:473–485, 2002.

[7] S. B. Cummins, P. Lonergan, A. C. O. Evans, and S. T. Butler. Genetic merit for fertility traits in Holstein cows: II. Ovarian follicular and corpus luteum dynamics, reproductive hormones, and estrus behaviour. *J. Dairy Sci.*, 95(7):3698–3710, 2012.

[8] L.A. Harris. *Differential equation models for the hormonal regulation of the menstrual cycle*. PhD thesis, North Carolina State University, 2001.

[9] K. Heinze, R.W. Keener, and A.R. Midgley. A mathematical model of luteinizing hormone release from ovine pituitary cells in perifusion. *Am. J. Physiol. Endocrinol. Metab.*, 275:1061–1071, 1998.

[10] R.L. Larson and R.F. Randle. The bovine estrous cycle and synchronization of estrus. `http://www.vet.ksu.edu/studentorgs/bovine/pdf/Estrous_Cycle_physiology1.pdf`.

[11] S. Meier, J.R. Roche, E.S. Kolver, and R.C. Boston. A compartmental model desribing changes in progesterone concentrations during the estrous cycle. *J. Dairy Res.*, 76:249–256, 2009.

[12] G.D. Niswender, J.L. Juengel, P.J. Silva, M.K. Rollyson, and E.W. McIntush. Mechanisms controlling the function and life span of the corpus luteum. *Physiol. Rev.*, 80:1–29, 2000.

[13] A.B. Pleasants, J.F. Smith, T.K. Soboleva, A.J. Peterson, L.M. Chagas, and C.R. Burke. Relationships among metabolic hormones, luteinising hormone and anoestrus in periparturient dairy heifers fed two nutritional levels prepartum. *AgResearch Limited Report*, 65:329–334, 2005.

[14] J.E. Pryce, M. Royal, P.C. Garnsworthy, and I.L. Mao. Fertility in the high-producing dairy cow. *Livest. Prod. Sci.*, 86:125–135, 2004.

[15] J.F. Smith, T.K. Soboleva, A.J. Peterson, A.B. Pleasants, L.M. Chagas, and C.R. Burke. Mathematical modelling of anoestrus in dairy cows and the linkage to nutrition. In *Proceedings of the New Zealand Society of Animal Production*, volume 65, pages 324–328, 2005.

[16] T.K. Soboleva, A.J. Peterson, A.B. Pleasants, K.P. Mc Natty, and F.M. Rhodes. A model of follicular development and ovulation in sheep and cattle. *Anim. Reprod. Sci.*, 58:45–57, 2000.

[17] J.L. Stevenson, J.C. Dalton, J.E. Santos, R. Sartori, A. Ahmadzadeh, and R.C. Chebel. Effect of synchronization protocols on follicular development and estradiol and progesterone concentrations of dairy heifers. *J. Dairy Sci.*, 91(8):3045–3056, 2008.

[18] C. Stötzel, J. Plöntzke, and S. Röblitz. Advances in modelling of the bovine estrous cycle : Administration of prostaglandin F2α. *Theriogenology*, 2012. Accepted for publication. Preprint available at `http://opus4.kobv.de/opus4-zib/frontdoor/index/index/docId/1274`.

[19] M. Wiltbank, H. Lopez, R. Sartori, S. Sangsritavong, and A. Gümen. Changes in reproductive physiology of lactating dairy cows due to elevated steroid metabolism. *Theriogenology*, 65:17–29, 2006.